Charge Regulation of Interacting Weak Polyelectrolytes

Yoram Burak*

School of Physics and Astronomy, Raymond and Beverly Sackler Faculty of Exact Sciences, Tel Aviv University, Tel Aviv 69978, Israel

Roland R. Netz

Sektion Physik, LMU Munich, Theresienstrasse 37, 80333 Munich, Germany

Received: August 9, 2003; In Final Form: December 2, 2003

We introduce a generalized nonuniform mean-field formalism to describe the dissociation of weak rodlike polyelectrolytes (PEs). Our approach allows for two-sublattice symmetry breaking which in titration curves is associated with a plateau for intermediate dissociation degrees. We first test our method in the case of a single weak PE by comparison with exact enumeration studies and show that it gives quantitatively accurate results for the dissociation degree in the full range of pH values and specifically performs much better than the nearest-neighbor approximation (where exact solutions are possible). We then study charge regulation of the coupled system of a weak polyacid and a weak polybase as a function of their mutual distance, which has some relevance for PE multilayer formation and for PE complexation. An intricate interplay of the degree of dissociation and the effective interaction between the PEs as a function of their mutual distance is found.

I. Introduction

The charge of weak polyacids and polybases is determined by the probability of each functional group to dissociate and expose a charged residue. This probability depends on a chemical equilibrium that can be tuned by varying the pH of the solution. In contrast to dilute solutions of monoacids or monobases, in weak polyelectrolytes (PEs) each functional group is influenced by all other groups along the polymer, via their mutual electrostatic interaction. As a result of the repulsion between charged groups, even strong PEs become weak at low salt concentrations. Furthermore, when two or more polymers interact with each other, their degree of ionization is modified, compared to their isolated state, and depends on parameters such as the distance between the polymers and their relative spatial configuration. Due to the many-body nature of this problem, and the long range of the electrostatic interactions, an exact solution for the average charge as function of pH is generally not known.

In this paper we consider stiff PEs, where there is no coupling between the dissociation degree of freedom and the polymer conformation (for treatment of such coupling in flexible PEs see, for example, refs 1−3). We consider first a single PE in salt solution and discuss some of the approximations commonly used to characterize its charge regulation. It was previously shown that a uniform mean-field approach cannot adequately describe charge regulation when the coupling between charges along the polymer is strong.[4] In these cases ionizable groups dissociate in a two-step process, characterized by a plateau in the charge vs pH curve. This process results from a spatially inhomogeneous charging pattern and is not predicted by a uniform mean-field approach. We introduce a mean-field theory with explicit symmetry breaking between two sublattices. Such an approximation is shown to be semiquantitatively accurate and performs better than previous calculations where the range of interactions is restricted,[4] as we demonstrate by comparison with exact enumeration over all configurations for finite chain lengths.

In the second part of the paper we apply our nonuniform mean-field scheme to the interaction of two stiff PEs. We restrict ourselves to the simple case of polymers aligned parallel to each other and calculate the average charging and free energy as a function of their distance. Our model reveals some of the intricate effects that can occur in interacting weak PEs. In a broader context, these interactions are of interest in the formation of PE multilayers, composed of alternating layers of positively and negatively charged polymers.[5−7] In particular, weak polyacids and polybases can be used to form multilayers.[8,9] In this case properties such as the layer thickness and density depend strongly on the dissociation degree of the functional groups and can be tuned sensitively by varying the pH of the solution.[9]

II. Single Polyelectrolyte

The free energy for a weak PE, immersed in an aqueous ionic solution, can be written as follows:

$$F = -\ln \sum_{\{s_i=0,1\}} \exp(-\mathscr{H}) \tag{1}$$

The Hamiltonian $\mathscr{H}$ is given by

$$\mathscr{H} = \mu \sum_i s_i + \sum_{i>j} s_i s_j v_{\mathrm{DH}}(\mathbf{r}_i, \mathbf{r}_j) \tag{2}$$

where r_i is the position of the ith monomer and s_i can be either zero (for an uncharged monomer) or one (charged monomer). The sum in eq 1 goes over all different configurations of dissociated groups. Note that F and $\mathscr{H}$ are given in units of the thermal energy $k_B T$. The chemical potential μ is related to the

* Corresponding author. E-mail: yorambu@post.tau.ac.il.

10.1021/jp036367i CCC: $27.50
Published on Web 03/20/2004

pH of the solution:[10]

$$\mu = -2.303(\mathrm{pH} - \mathrm{p}K_a) - l_B\kappa \qquad \text{(acid)}$$
$$\mu = 2.303(\mathrm{pH} - \mathrm{p}K_b) - l_B\kappa \qquad \text{(base)} \tag{3}$$

where κ is the Debye screening length, $l_B = e^2/(\epsilon k_B T)$ is the Bjerrum length, equal to about 7 Å in water at room temperature, $k_B T$ is the thermal energy, ϵ_w is the dielectric constant of water, and e is the unit charge. The last term in eq 3 is the self-energy of the two charges created in the dissociation process. We assume throughout this paper that the ionic solution can be described using the linearized Debye−Hückel theory, so that electrostatic interactions between charges are pairwise additive, as in eq 2. The exact form of v_{DH} depends on the salt concentration, and also on the dielectric properties of the polymer backbone, as will be discussed below. In the most simple case of dielectric continuity between the polymer and solution, v_{DH} is equal to

$$v_{DH}(\mathbf{r}_1,\mathbf{r}_2) = l_B \frac{e^{-\kappa|\mathbf{r}_1-\mathbf{r}_2|}}{|\mathbf{r}_1-\mathbf{r}_2|} \tag{4}$$

The linear Debye−Hückel approach neglects nonlinear effects that are associated with counterion condensation and which are contained in the nonlinear Poisson−Boltzmann formalism. The main reason for resorting to linear theory is that only at that level can the complicated problem of spatially inhomogeneous charge distributions on the PE backbone be calculated. One justification is that weak polyelectrolytes as studied in this paper are typically not strongly charged, so that nonlinear effects are less important than for strong polyelectrolytes, as will be discussed in more detail in the concluding section.

For the following calculations, it is convenient to use symmetric variables $\tilde{s}_i$ having the values -1, $+1$ instead of 0, 1:

$$s_i = \frac{1+\tilde{s}_i}{2} \tag{5}$$

In terms of these variables the partition function is

$$Z = \sum_{\{\tilde{s}_i=-1,+1\}} \exp\{-\tilde{c} - \tilde{\mu}\sum_i \tilde{s}_i - \sum_{i>j}\tilde{s}_i\tilde{s}_j\tilde{v}_{DH}[a(i-j)]\} \tag{6}$$

where

$$\tilde{c} = \frac{1}{2}N\mu + \frac{1}{4}N\sum_{j>0} v_{DH}[aj]$$
$$\tilde{\mu} = \frac{\mu}{2} + \frac{1}{2}\sum_{j>0} v_{DH}[aj]$$
$$\tilde{v}_{DH} = \frac{1}{4}v_{DH} \tag{7}$$

and a is the nearest-neighbor distance between dissociable groups on a straight line.

A. Nonuniform Mean-Field Approach with Two Sublattices. *1. Mean-Field Equations.* In principle, the above statistical one-dimensional problem can be solved using transfer-matrix techniques that take the long-range interactions into account via a multiple-time integration with a suitably chosen kernel. To obtain a simple, tractable solution, we use mean-field methods, which are implemented in the following way. The Gibbs variational principle can be used to obtain an upper bound for the free energy $F = -\ln Z$,

$$F \le F_0 + \langle \mathscr{H} \rangle_0 - \langle \mathscr{H}_0 \rangle_0 \tag{8}$$

In this inequality $\mathscr{H}_0$ is a trial Hamiltonian (to be specified below) and $F_0 = -\ln Z_0$, where Z_0 is the partition function obtained from $\mathscr{H}_0$. The thermal averages in eq 8 are evaluated using $\mathscr{H}_0$. We introduce the trial Hamiltonian

$$\mathscr{H}_0 = h_0\sum_i \tilde{s}_{2i} + h_1\sum_i \tilde{s}_{2i+1} \tag{9}$$

which separates the polymer into two sublattices. The variational parameters h_0, h_1 are fields that act on the charges in the two sublattices. By minimizing the right-hand side of eq 8 with respect to h_0 and h_1, the following equations are obtained,

$$h_0 = \tilde{\mu} + J\langle\tilde{s}_0\rangle_0 + K\langle\tilde{s}_1\rangle_0$$
$$h_1 = \tilde{\mu} + J\langle\tilde{s}_1\rangle_0 + K\langle\tilde{s}_0\rangle_0 \tag{10}$$

where

$$\langle\tilde{s}_0\rangle_0 = -\tanh(h_0) \qquad \langle\tilde{s}_1\rangle_0 = -\tanh(h_1) \tag{11}$$

and

$$J = \frac{1}{2}\sum_{j>0} v_{DH}[2ja] \qquad K = \frac{1}{2}\sum_{j\ge 0} v_{DH}[(2j+1)a] \tag{12}$$

The choice of two sublattices (as opposed to more sublattices with a larger period) is related to the strong anticorrelation that can exist between adjacent monomers and will be further motivated below.

2. Main Properties of Mean-Field Equations. Equations 10 and 11 always have a symmetric solution for which $h_0 = h_1$. However, the symmetric solution is not always the minimum of the free energy but can be, instead, a saddle point in the 2D plane spanned by h_0 and h_1. In these cases two other solutions exist, both of which break the symmetry between the two sublattices, i.e., $h_0 \neq h_1$. One solution can be obtained from the other by exchanging h_0 and h_1. The average charging degree of the polymer is then equal to

$$\langle s\rangle_0 = \frac{\langle\tilde{s}\rangle_0 + 1}{2} = \frac{\langle\tilde{s}_0\rangle_0 + \langle\tilde{s}_1\rangle_0 + 2}{4} \tag{13}$$

To understand for which parameters symmetry breaking occurs, let us consider first the case $\tilde{\mu} = 0$. In this case the Hamiltonian exhibits the symmetry $\tilde{s}_i \rightarrow -\tilde{s}_i$ in addition to the symmetry of exchanging the two sublattices. Even if the latter symmetry is broken, we have $\langle\tilde{s}\rangle_0 = 0$, or equivalently, $\langle s\rangle_0 = {}^1/_2$, i.e., exactly half of the monomers are dissociated. Using the fact that $h_0 = -h_1$, eqs 10 and 11 reduce in this case to one transcendental equation,

$$h_0 = (K - J)\tanh(h_0) \tag{14}$$

This equation has a nonzero solution (where $h_0 \neq h_1$) only if

$$K - J > 1 \tag{15}$$

If this condition is met, a sublattice symmetry breaking solution also exists within a certain range of $\tilde{\mu}$ values around zero. Outside the range $|\tilde{\mu}| < \tilde{\mu}_c$ there is no symmetry breaking,

i.e., $\langle \tilde{s}_0 \rangle_0 = \langle \tilde{s}_1 \rangle_0$. If condition (15) is not met, there is no symmetry breaking solution for any value of $\tilde{\mu}$.

The solution with $h_0 = h_1$ (no sublattice symmetry breaking) can be found by substituting this equality in eqs 10 and 11, leading to the transcendental equation

$$h_0 = (K + J) \tanh(h_0) \tag{16}$$

In a uniform mean-field approximation this solution is found for all values of $\tilde{\mu}$, whereas in our case it applies only for $|\tilde{\mu}| \geq \tilde{\mu}_c$.

Before considering concrete examples we comment on the nature of the transition at $\tilde{\mu} = \pm\tilde{\mu}_c$. This transition is second order, i.e., $\langle \tilde{s}_1 \rangle_0 - \langle \tilde{s}_0 \rangle_0 \to 0$ as $\tilde{\mu} \to \pm\tilde{\mu}_c$. Note that a nonzero $\tilde{\mu}$ does not break the symmetry of exchanging the two sublattices in the Hamiltonian. This is why the order parameter is continuous at the transition. However, the derivative of the order parameter with respect to $\tilde{\mu}$ is discontinuous and diverges when approaching the transition from the side where symmetry breaking occurs. Similarly, the derivative of the average dissociation degree with respect to $\tilde{\mu}$ has a discontinuity at the transition. These are artifacts of the mean-field approach, because the exact solution for a one-dimensional system with short-range interactions cannot exhibit a real phase transition.[11] However, our nonuniform mean-field scheme still predicts the average charge very accurately, as will be demonstrated below.

B. Uniform Dielectric Constant. In the case of a uniform dielectric constant, in which the screened interaction is given by eq 4, the summations in eq 12 can be performed explicitly, yielding

$$J = -\frac{l_B}{4a}[\ln(1 - e^{-\kappa a}) + \ln(1 + e^{-\kappa a})]$$

$$K = -\frac{l_B}{4a}[\ln(1 - e^{-\kappa a}) - \ln(1 + e^{-\kappa a})] \tag{17}$$

$$\tilde{\mu} = \frac{\mu}{2} - \frac{l_B}{2a}\ln(1 - e^{-\kappa a}) \tag{18}$$

The condition for sublattice symmetry breaking, eq 15, translates to

$$K - J = \frac{l_B}{2a}\ln(1 + e^{-\kappa a}) > 1 \tag{19}$$

Increasing κ decreases $K - J$ and thus the possibility for sublattice symmetry breaking. Symmetry breaking can occur for a finite range of κ and pH only if the condition

$$\frac{l_B}{a} > \frac{2}{\ln 2} \simeq 2.9 \tag{20}$$

is met. For $l_B = 7.0$ Å this condition leads to $a \lesssim 2.4$ Å. Hence vinyl-based polymers with an acid group on every second carbon atom such as poly(styrenesulfonate) or poly(acrylic acid) with a charge distance of $a \approx 2.5$ Å are marginally close to symmetry breaking within the present model. However, a dielectric discontinuity due to the polymer backbone can increase $K - J$ considerably, as will be discussed in the following subsection.

Examples with symmetry breaking will be shown in the following subsection, whereas here we restrict ourselves to the case of dielectric continuity and no symmetry breaking. In the case of no symmetry breaking all the dependence on κ enters through the quantity

$$K + J = -(l_B/2a)\ln(1 - e^{-\kappa a}) \tag{21}$$

which increases with increasing Debye length κ^{-1}.

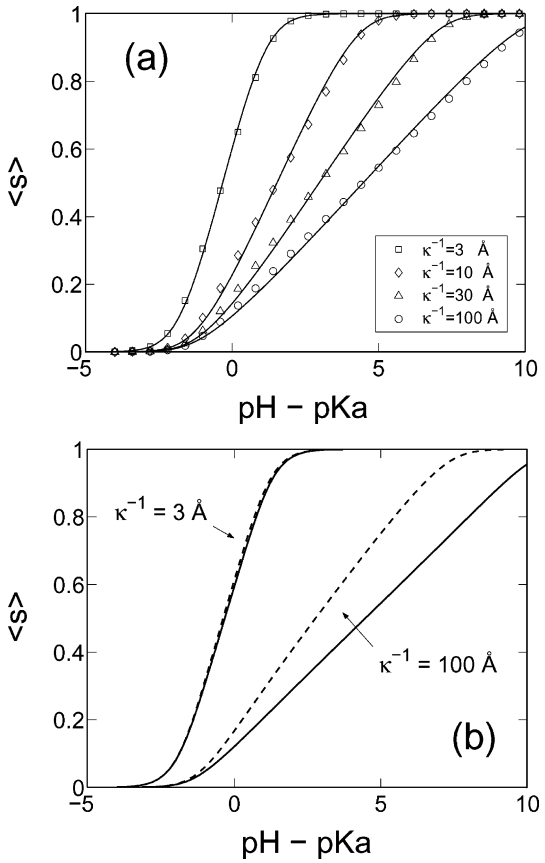

Figure 1. (a) Average degree of dissociation of a polyacid as a function of pH − pK_a, calculated using a mean-field approximation (solid lines). For comparison an exact enumeration over all configurations is also shown (symbols) with $N = 20$ and using periodic boundary conditions. Results for four different values of the Debye length are shown, $\kappa^{-1} =$ 3 Å (squares), 10 Å (diamonds), 30 Å (triangles), and 100 Å (circles). The separation between charged groups is $a = 2.5$ Å. (b) Average degree of dissociation as function of pH − pK_a, calculated using an exact enumeration for a chain length $Na = 50$ Å. The solid lines show enumeration results with periodic boundary conditions (as shown using symbols in (a)). These results are compared with enumeration without periodic boundary conditions (dashed lines). Two different values of the Debye length are shown in the plot, $\kappa^{-1} = 3$ Å (to the left) and 100 Å (to the right).

1. Results. In Figure 1a we show the average degree of charge dissociation following from our mean-field equation for a polyacid with $a = 2.5$ Å, for four different salt concentrations, corresponding to $\kappa^{-1} = 3$, 10, 30, and 100 Å (solid lines). These results are compared with an exact calculation of the free energy for a finite chain with $N = 20$ dissociable groups (symbols), by enumeration over all 2^N states. For the exact enumeration, periodic boundary conditions are imposed by setting the interaction between monomers i and j to be

$$v^p_{DH}(i,j) = \sum_{n=-\infty}^{\infty} v_{DH}(i,j+nN) \tag{22}$$

The comparison between mean-field and the exact enumeration is very good for all four values of κ^{-1} shown in the figure. Note that in all these cases there is no symmetry breaking in the mean-field solution, as expected because the charge distance of $a = 2.5$ Å does not satisfy the condition eq 20. Comparison

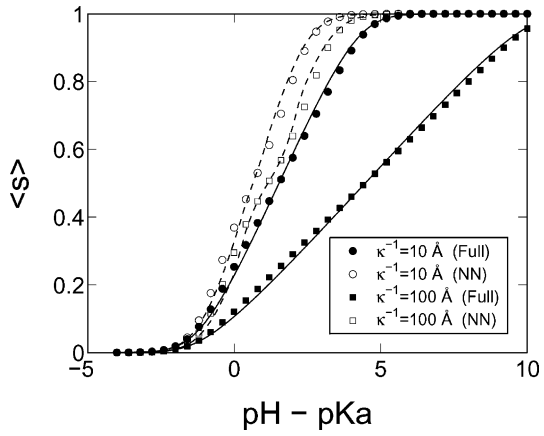

Figure 2. Comparison of a nearest-neighbor mean-field approximation (dashed lines) with a mean-field calculation taking into account all long-range interactions (solid lines) for a polyacid having $a = 2.5$ Å, as a function of pH − pK_a. Results for two values of the Debye length are shown. They can be distinguished in the plot according to the type of symbols (circles, $\kappa^{-1} = 10$ Å; squares, $\kappa^{-1} = 100$ Å). The symbols show exact enumeration results with $N = 20$ and periodic boundary conditions (empty symbols, only nearest-neighbor interactions; full symbols, full long-range interaction). In the enumeration with NN interactions results are nearly identical to the analytical expression for an infinite chain.

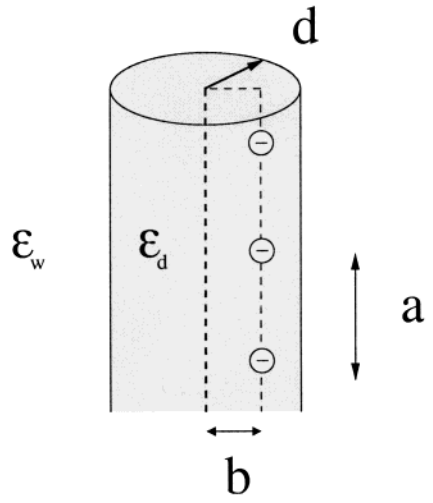

Figure 3. Schematic representation of a simple model taking into account the difference between the dielectric properties of water and a polymer's backbone. A PE is modeled as a cylinder of radius d with a dielectric constant ϵ_d, whereas the dielectric constant outside the cylinder is equal to ϵ_w. Charged groups that can dissociate from the polymer are located at regular intervals a from each other, at a distance b from the cylinder axis.

of the four curves shows that κ^{-1} has a large effect on the degree of charging. As κ^{-1} is increased, each monomer interacts more strongly with the other monomers. This increased repulsion reduces the charging, or, as one might put it, the long-range repulsion between charged groups makes even strong PEs weak.

Throughout this work we will assume that the polymer is long compared to the Debye length. However, it is important to realize that for shorter polymers the average degree of dissociation depends on the polymer length. To demonstrate this point, we show in Figure 1b the average degree of dissociation as function of pH for a finite chain of length Na, where $N = 20$ and $a = 2.5$ Å. In the calculation an exact enumeration over all configurations is performed, without periodic boundary conditions (dashed lines). The results are compared with an enumeration with periodic boundary conditions (solid lines), as was done in Figure 1a. For $\kappa^{-1} = 3$ Å, the polymer length is larger than the screening length, $Na \gg \kappa^{-1}$ and the two calculations yield nearly identical results. In the second case shown in the plot, $\kappa^{-1} = 100$ Å, κ^{-1} and Na are of the same order of magnitude and there are significant finite size effects. These results may be important for the interaction of short DNA oligomers with substrates, as they show that the polymer length affects adsorption behavior also via the effective charge of PEs.

2. Restriction to Nearest-Neighbor Interactions. A common approximation that was previously applied for the charge regulation of PEs is to consider only nearest-neighbor (NN) interactions.[12−14] The reason is that exact closed-form solutions are available in this case. Within the nonuniform mean-field approach, this approximation corresponds to setting $K = (l_B/2a)\exp(-\kappa a)$ and $J = 0$. Note that the combination $K + J$, which determines the solution without symmetry breaking, is smaller in the NN case than in full interaction case. On the other hand the combination $K - J$, which affects the symmetry breaking (see eq 15), is larger in the NN case.

In Figure 2 we compare the NN predictions (dashed lines and open symbols) with those obtained using the full long-range interaction (solid lines and filled symbols), for two different values of the Debye length. The symbols show exact enumeration results, obtained using periodic boundary conditions and are thus representative of an infinitely long system, whereas the lines show mean-field results. For both values of the Debye length there are significant deviations between the NN result and the full interaction. As can be expected, these deviations are larger for the larger screening length, $\kappa^{-1} = 100$ Å, because in this case the interaction between further-nearest neighbors contributes significantly to the total interaction. Note that for $\kappa^{-1} = 100$ Å and NN interactions (open square symbols and dashed line) there is also a small effect of symmetry breaking in the mean-field solution, resulting in a nonmonotonic slope near $\langle s \rangle = 0.5$. A similar effect is seen in the exact enumeration. As a main result of this section, we see that the restriction to nearest-neighbor interactions is in general not a good approximation, whereas the mean-field approach reproduces the exact enumeration results very accurately.

C. Nonuniform Dielectric Constant. So far we neglected the effects of the dielectric discontinuity between the polymer and its surroundings. As these effects tend to increase the electrostatic interactions, they are expected to be important for the dissociation process. They were estimated in ref 4 using a simple model, shown in Figure 3. The PE is modeled as a cylinder of radius d and dielectric constant $\epsilon_d < \epsilon_w$, where $\epsilon_w \simeq 80$ is the dielectric constant of water. Charged groups are assumed to be equally spaced along the cylinder axis, with separation a. Here we generalize this model to some extent by placing these charged groups at a distance $0 \le b \le d$ from the axis, as shown in Figure 3. The electrostatic potential exerted by one such charge on another one was calculated in ref 4 and is given by

$$\psi = \frac{\epsilon_w}{\epsilon_d}\frac{l_B}{z} + \frac{1}{2\pi}\sum_{n=-\infty}^{\infty} W_p(z,n) \qquad (23)$$

where z is the distance between the charges. The first term is equal to the electrostatic interaction within a medium of dielectric constant ϵ_d, with no screening by salt. In the second term, W_p is equal to

$$W_p(z,n) = 4\frac{\epsilon_w}{\epsilon_d} l_B \int_0^\infty dk \cos(kz)[I_n(kb)]^2 R(k,n) \qquad (24)$$

where

$$R(k,n) = \frac{k\epsilon_d[K_{n-1}(kd) + K_{n+1}(kd)]K_n(pd) - p\epsilon_w[K_{n-1}(pd) + K_{n+1}(pd)]K_n(kd)}{k\epsilon_d[I_{n-1}(kd) + I_{n+1}(kd)]K_n(pd) + p\epsilon_w[K_{n-1}(pd) + K_{n+1}(pd)]I_n(kd)} \qquad (25)$$

$p = (k^2 + \kappa^2)^{1/2}$ and K_n, I_n are the nth modified Bessel functions of the first and second kind, respectively.

In ref 4 only the case $b = 0$ was considered. For two charges located exactly at the polymer axis, $b = 0$, the electrostatic interaction approaches $(\epsilon_w/\epsilon_d)l_B/z$ at short separations, whereas for larger separations it crosses over to the interaction in the aqueous ionic solution, $l_B \exp(-\kappa z)/z$. The former interaction is typically much larger than the latter, leading to a two-step charging curve and failure of a uniform mean-field approach. On the other hand, only close-by monomers interact strongly with each other, motivating the use of a nearest-neighbor (NN) model,[4] where only interactions between neighboring monomers are taken into account. The free energy and average degree of dissociation can then be calculated exactly,[12,13,14] e.g., using the transfer matrix method.[11,15]

The NN approximation indeed predicts the two-step behavior of the charging curve, but it can fail for large values of the Debye screening length, because in this case further−nearest-neighbor interactions become important. For large κ^{-1} long-range interactions can be important although they are much weaker than the interactions between neighboring monomers, as shown in the following numerical examples.

1. Results for Radially Symmetric Charge Distribution. In Figure 4a the NN prediction (dashed line, exact solution) is compared with an enumeration using the full long-range interaction (circles). The Debye length is $\kappa^{-1} = 100$ Å, and interactions between monomers are calculated using eq 23 with $b = 0$, $d = 2.5$ Å, $\epsilon_w/\epsilon_d = 80/3$ and a monomer separation $a = 3.5$ Å. In all calculations with dielectric discontinuity we use a monomer separation $a = 3.5$ Å rather than 2.5 Å, which corresponds to a somewhat smaller fraction of dissociable groups.

The exact solution of the NN model in Figure 4a (broken line) deviates significantly from the enumeration results with the full range of interactions included (circles). In contrast, our nonuniform mean-field approach with symmetry breaking (solid line in Figure 4a) is semiquantitatively correct. The success of our generalized mean-field approximation is one of the main results in the first part of this work. Note that the main difference with respect to enumeration is that the mean-field approximation over-estimates the effects of symmetry breaking, as seen from the exaggerated size of the plateau region.

We also present in Figure 4a a comparison between the NN exact solution (dashed line) and an enumeration taking only nearest-neighbor interactions into account (crosses). This is done to test finite size effects in the exact enumeration. The enumeration and exact solution yield almost identical results, demonstrating that an enumeration with $N = 20$ is typically very accurate for a single polymer. We note that periodic boundary conditions are essential to obtain this level of accuracy in enumeration, when long-range interactions are included (compare Figure 1b). As another test for the enumeration procedure we increased N to 30 for several different choices of $\upsilon_{DH}(z)$. In all these cases deviations from results with $N = 20$ were insignificant.

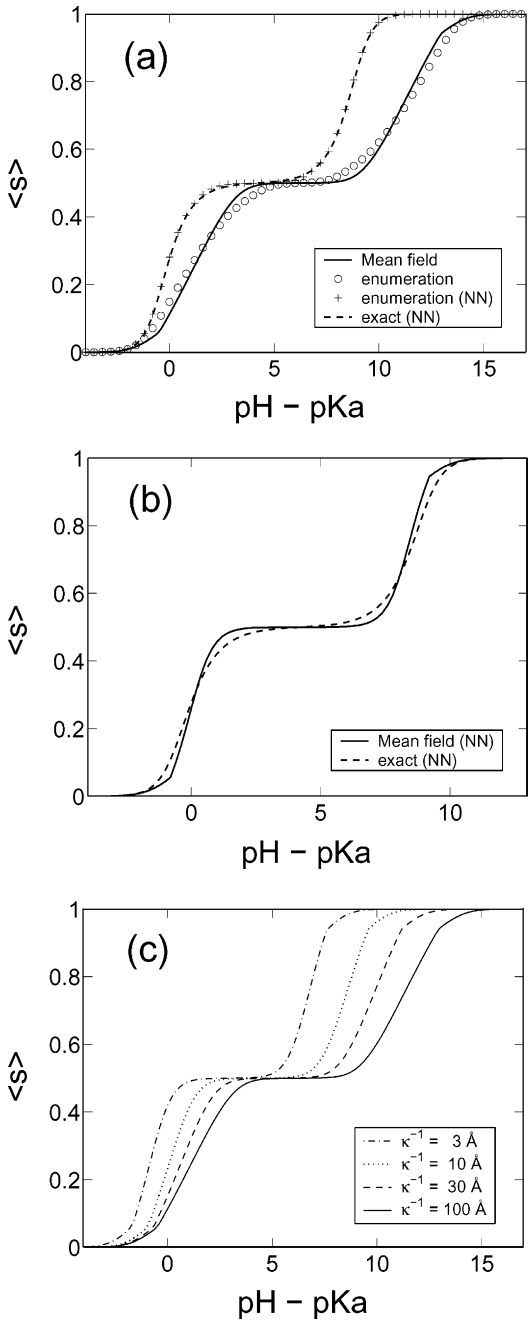

Figure 4. Average degree of dissociation of a polymer with strong interactions between close-by monomers, characterized by a plateau near $\langle s \rangle = 1/2$. The interactions between monomers are calculated using the cylindrical model shown in Figure 3, with $\epsilon_d = 3$, $\epsilon_w = 80$, $d = 2.5$ Å, $a = 3.5$ Å, $b = 0$, and a Debye length $\kappa^{-1} = 100$ Å. (a) Mean-field results with two sublattices (solid line) are compared with an enumeration over all configurations with $N = 20$ and periodic boundary conditions (circle symbols). The mean-field results show two cusps, where transitions occur between a solution with no symmetry breaking and one with symmetry breaking (the latter occurs for intermediate pH). Results are also compared with an enumeration taking only nearest-neighbor (NN) interactions into account (crosses) and the exact solution with NN interactions, calculated using the transfer matrix method (dashed line). (b) Mean-field calculation with two sublattices taking only NN interactions into account (solid line), compared with the exact solution with NN interactions (dashed line). (c) Dissociation as a function of PH for four different values of the Debye screening length: $\kappa^{-1} = 3$, 10, 30, and 100 Å, calculated using the mean-field approximation with two sublattices. All parameters other than κ are as in part (a). The interaction parameters J, K used in the mean-field approximation are equal to 0.21, 4.36 ($\kappa^{-1} = 3$ Å); 0.46, 4.86 ($\kappa^{-1} = 10$ Å); 0.87, 5.30 ($\kappa^{-1} = 30$ Å); and 1.37, 5.84 ($\kappa^{-1} = 100$ Å).

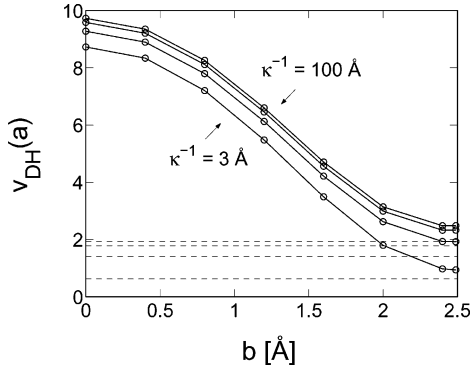

Figure 5. Dependence of the electrostatic interaction between two monomers on their distance b from the polymer axis, within the cylindrical model of Figure 3. The distance between the monomers is $a = 3.5$ Å, and the other model parameters are $d = 2.5$ Å, $\epsilon_d = 3$ and $\epsilon_w = 80$. Results are shown for four values of the Debye length, $\kappa^{-1} =$ 3, 10, 30, and 100 Å. The electrostatic interaction in an aqueous ionic solution is shown for comparison using dashed lines.

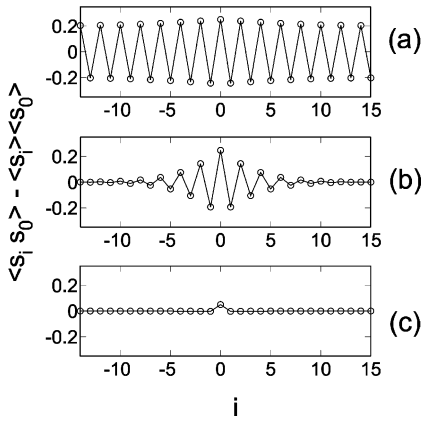

Figure 6. Correlation function between the dissociation of a monomer and that of its neighbors, $\langle s_i s_0 \rangle - \langle s_i \rangle \langle s_0 \rangle$, calculated from an exact enumeration over all configurations of a PE having $N = 30$ monomers, with periodic boundary conditions. All physical parameters are as in Figure 4a. The pH is equal to 7 in (a), corresponding to $\tilde{\mu} = 0$, to 9 in (b), and to 13.5 in (c).

Figure 4b shows a comparison between the NN exact solution (broken line) and a mean-field calculation with two sublattices (solid line), taking only the NN interaction into account, for $\kappa^{-1} = 100$ Å. The NN mean-field approximation shows an effect similar to the curve in Figure 4a: two artificial discontinuities in the derivative of $\langle s \rangle$ are seen, corresponding to two erroneous second-order transitions. In addition, the plateau is more pronounced compared to the exact solution. Nevertheless, the overall prediction for $\langle s \rangle$ as function of pH is quite accurate.

Finally, the dependence on the Debye screening length κ^{-1} is investigated in Figure 4c, using our nonuniform mean-field approach. The parameters J and K of the sublattice interactions are calculated for each value of κ using eqs 12 and 23. For all four values of κ^{-1} shown, $\kappa^{-1} = 3$, 10, 30, and 100 Å, a pronounced plateau is visible. The cusps that are present in all four cases (for example, at $\langle s \rangle \simeq 0.07$ and $\langle s \rangle \simeq 0.93$ in (a)) are artifacts due to the mean-field approach.

2. Dependence on the Position of Charged Groups. In most polyacids and polybases the charged units are located in side groups, rather than being close to the polymer axis. This raises the question whether an interaction much larger than the usual Debye−Hückel interaction will occur even if the charges are displaced from the axis. Within the simple cylindrical model presented above, this question can be addressed by calculating the electrostatic interaction between two monomers as a function of b. Such a calculation is shown in Figure 5, for four different values of the screening length κ^{-1}. The monomers are separated by a distance of $a = 3.5$ Å, and the polymer radius is taken as $d = 2.5$ Å, as in Figure 4. In all four cases a very large decrease of υ_{DH} occurs with an increase of b toward the cylinder boundary, $b = d$. For large d this result is not surprising, because the cylinder becomes similar to a planar interface, separating an aqueous ionic solution and a low dielectric medium. Near such an interface the electrostatic interaction is equal to twice the screened electrostatic interaction in water.[16] For large cylinder radius $d \gg \kappa^{-1}$ we have checked that eq 23 indeed yields this result. In Figure 5 the cylinder radius is not large compared to the Debye length and the interaction close to the cylinder boundary is even smaller than in the planar limit. The screened interaction in water is shown for comparison using dashed lines.

The above analysis demonstrates that actual electrostatic interactions between nearby monomers depend strongly on the spatial organization of the PE. These interactions probably cannot be estimated reliably using simplified models such as the cylindrical one presented above. The detailed polymer structure, as well as other effects such as the discreteness of the solvent, must be taken into account.

D. Further Discussion of the Two-Sublattice Approximation. Although the comparison with exact enumeration demonstrates that a two-sublattice model is useful, one may ask to what extent the separation into two sublattices has a physical significance. To discuss this question, we note that within the plateau region of the titration curve there is typically a strong anticorrelation between even and odd monomers. To understand this anticorrelation, one may think of the ground state of the Hamiltonian in eq 6, concentrating first on the special case $\tilde{\mu} = 0$. When the interaction between monomers favors opposite dissociation values, the ground state is typically a periodic array of alternating values in the even and odd positions, $s = +1$ and $s = -1$. The long-range order of the ground state is not preserved within the exact theory at any finite temperature, due to the entropy associated with domain boundaries in a one-dimensional system.[11] Nevertheless, at a certain range of pH values around $\tilde{\mu} = 0$, we may expect a staggered correlation function with strong anticorrelation between even and odd monomers.

As an example, Figure 6 shows the correlation function, $\langle s_i s_0 \rangle - \langle s_i \rangle \langle s_0 \rangle$, for a PE having the same parameters as in Figure 4a, calculated by exact enumeration over all states of a PE of length $N = 30$ and using periodic boundary conditions. Results are shown for three different pH values: in the top plot, pH = 7, corresponding to $\tilde{\mu} = 0$. The correlation function has a staggered form, which persists over the full length of the PE. Nevertheless, it is clear that there is no true long-range order because the (anti) correlation decreases slightly with monomer separation. In the middle plot, where the pH is equal to 9, the correlation has a shorter range, persisting only up to a distance of about 8 sites from the center monomer. Note that a pH value of 9 is approximately at the right edge of the plateau region seen in Figure 4a. With a further increase of pH the correlation length continues to decrease and at pH = 13.5 (bottom plot) there is almost no correlation even between adjacent monomers. This pH value is close to the transition point that is found in the two-sublattice model, beyond which there is no symmetry breaking between the two sublattices. In summary, Figure 6 demonstrates that the two-sublattice approximation captures an essential physical property of the dissociation pattern that is

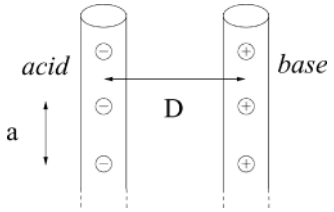

Figure 7. Schematic illustration of a model describing the interaction of a polyacid with a parallel polybase, separated by a distance *D*. The distance between charged groups in both of the PEs is *a*. For simplicity the charged groups are facing each other.

absent in the uniform mean-field approach, namely, a strong anticorrelation between even and odd sites.

In principle, a periodicity other than 2 may be included in the formulation of the mean-field equations, and could lead, for certain parameters, to a lower free energy than the 2-fold periodicity. In such cases a plateau would be expected in the titration curve at an average degree of dissociation other than one-half. Comparison with the exact enumeration and with typical experimental results indicates that such additional symmetry breaking into structures with more than two sublattices does not occur within the physical parameters considered in this work.

In the second part of this work, where we will look at the interaction between two weak polyelectrolytes, we will employ Debye−Hückel interactions in a uniform dielectric constant, eq 4, as well as the interaction within a cylindrical dielectric cavity with $b = 0$, which constitute the two extreme cases. In both cases we expect a mean-field approach with two sublattices to be adequate to predict the average charging, as was demonstrated in the preceding discussion.

III. Interaction between Polyacid and Polybase

A. Uniform Mean-Field Approach. The model we consider is shown schematically in Figure 7. A polyacid (left) and polybase (right) are aligned parallel to each other and separated by a distance *D*. For simplicity we assume that the distance between charged groups (denoted by *a*) is identical in the two polymers and that the charge lattices are in phase with each other in the two polymers, as shown in the figure. We would like to calculate the average charge on the two polymers and the free energy as a function of *D*.

We consider first the case of a uniform dielectric constant, eq 4, and also assume that for each polymer a uniform mean-field theory (with no symmetry breaking) is adequate. As was shown in the calculations for a single polymer, the latter assumption is justified for monovalent monomers having a nearest-neighbor separation $a \gtrsim 2.5$ Å.

It is convenient to define for the polyacid

$$s_a = \frac{1 + \tilde{s}_a}{2} \tag{26}$$

and for the polybase

$$s_b = \frac{1 - \tilde{s}_b}{2} \tag{27}$$

where s_a and s_b are zero for an uncharged monomer and one for a charged (dissociated) one. With these definitions both $\tilde{s}_a$ and $\tilde{s}_b$ increase with pH.

The mean-field equations are found in a similar way as in the single polymer case and are given by

$$\begin{aligned} h_a &= \tilde{\mu}_a + J\langle\tilde{s}_a\rangle_0 + K\langle\tilde{s}_b\rangle_0 \\ h_b &= \tilde{\mu}_b + J\langle\tilde{s}_b\rangle_0 + K\langle\tilde{s}_a\rangle_0 \end{aligned} \tag{28}$$

where

$$\langle\tilde{s}_a\rangle_0 = -\tanh(h_a) \qquad \langle\tilde{s}_b\rangle_0 = -\tanh(h_b) \tag{29}$$

The coefficients in these equations are given by

$$\begin{aligned} J &= \frac{1}{4}\sum_{i\neq 0} v_{DH}(ia) \\ K &= \frac{1}{4}\sum_{i} v_{DH}[\sqrt{(ia)^2 + D^2}] \\ \tilde{\mu}_a &= -\frac{2.303}{2}(\mathrm{pH} - \mathrm{p}K_a) + \Delta\tilde{\mu} \\ \tilde{\mu}_b &= -\frac{2.303}{2}(\mathrm{pH} - \mathrm{p}K_b) - \Delta\tilde{\mu} \end{aligned} \tag{30}$$

where

$$\Delta\tilde{\mu} = \frac{1}{4}\sum_{i\neq 0} v_{DH}(ia) - \frac{1}{4}\sum_{i} v_{DH}(\sqrt{(ia)^2 + D^2}) - \frac{l_B\kappa}{2} \tag{31}$$

Equations 28 and 29 are very similar to eqs 10 and 11, with a number of important differences. First, the subscripts a and b do not represent two sublattices but instead distinguish between the polyacid and polybase. Another difference is that the chemical potentials $\tilde{\mu}_a$ and $\tilde{\mu}_b$ are usually not equal to each other. Most importantly, *J* is almost always larger than *K*, whereas for the two-sublattice case *J* is smaller than *K*. It is easy to show that for $J > K$ eqs 28 and 29 have a single solution.

1. Results. The electrostatic interaction between the polyacid and polybase increases dissociation in both polymers (in contrast to the interactions within each PE, which inhibits charged groups from dissociating). Figure 8 shows the degree of charging of a polyacid and polybase having $a = 2.5$ Å, as a function of pH and for three different values of *D*. When the polymers are sufficiently far away from each other, their dissociation curves are identical to those of a single polymer. For smaller separation the average charge increases. An important case occurs when the pH is tuned such that

$$(\mathrm{pH} - \mathrm{p}K_a) = -(\mathrm{pH} - \mathrm{p}K_b) \tag{32}$$

For example, with the parameters used in Figure 8, $\mathrm{p}K_a = 4$ (similar to poly(acrylic acid)) and $\mathrm{p}K_b = 10$ (similar to poly(vinylamine)), this equality holds at pH = 7. In this case, one has $\tilde{\mu}_b = -\tilde{\mu}_a$, as seen from eq 30, and the solution of eqs 28 and 29 has the properties $h_a = -h_b$ and $\langle\tilde{s}_a\rangle_0 = -\langle\tilde{s}_b\rangle_0$. Using the definitions in eqs 26 and 27, the average charging degrees of the polyacid and polybase are then equal to each other, and the value of h_a is found from the single transcendental equation:

$$h_a = \tilde{\mu}_a + (K - J)\tanh(h_a) \tag{33}$$

In the following examples we restrict ourselves to the symmetric case described by eqs 32 and 33. Figure 9a shows the average degree of dissociation as a function of the polymer separation *D* (identical for the polyacid and polybase). Results are shown for $a = 2.5$ Å, $\mathrm{pH} - \mathrm{p}K_a = \mathrm{p}K_b - \mathrm{pH} = 3$, and for four different values of the Debye length, ranging between 3 and 100 Å. When *D* is large compared to κ^{-1}, the polymers do

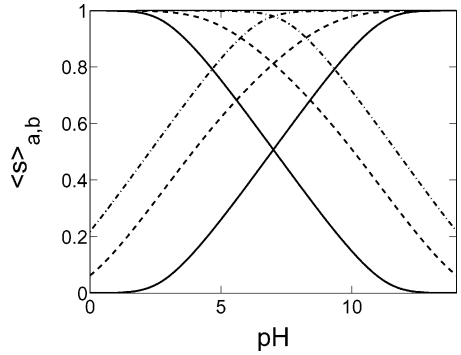

Figure 8. Average dissociation degree of a polyacid (increasing lines) interacting with a polybase (decreasing lines), as a function of pH. The distance between charges is $a = 2.5$ Å; $pK_a = 4$, $pK_b = 10$, and the Debye length is $\kappa^{-1} = 30$ Å. Results are shown for three values of the inter-polymer separation: $D = 100$ Å (solid lines), 10 Å (dashed lines), and 5 Å (dash−dot lines). The symmetric case where $pH - pK_a = pK_b - pH$ occurs at $pH = 7$.

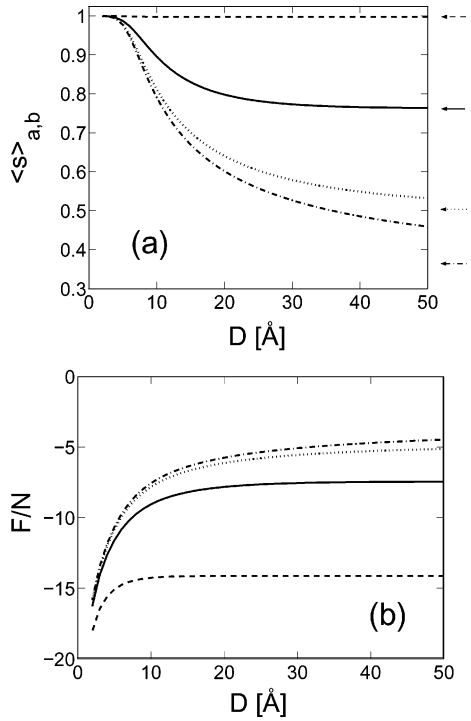

Figure 9. Average degree of dissociation (a) and free energy per monomer, F/N (b) as a function of the distance D between a polyacid and polybase, with $pH - pK_a = pK_b - pH = 3$. Simple Debye−Hückel interactions are used with $\kappa^{-1} = 3$ Å (dashed line), 10 Å (solid line), 30 Å (dotted line), and 100 Å (dash−dot line). All other parameters are as in Figure 8. The arrows on the right-hand side of (a) show the value of $\langle s \rangle$ for an isolated PE.

not interact, and their average charge is equal to its value in an isolated polymer (compare with Figure 2 at $pH - pK_a = 3$). This value depends strongly on κ^{-1}. At separations D of order κ^{-1} and smaller, the average charging increases with a decrease of D and approaches unity (full dissociation) at contact.

We turn to the free energy of the two interacting PEs, shown in Figure 9b. In this figure the free energy F is divided by N, the number of monomers in each PE. A distinctive feature in this figure is that F is almost independent of κ^{-1} at small separations. In contrast to this short separation behavior, F depends strongly on κ^{-1} at large separations. To understand these two behaviors, we consider each one of the two limits separately:

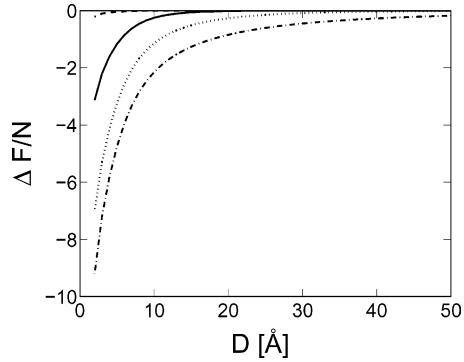

Figure 10. Difference ΔF between the free energy F of a polyacid interacting with a polybase, and the asymptotic form of eq 34. Four values of κ^{-1} are shown. These values, and all other parameters and notations are as in Figure 9. For each value of κ^{-1} the values of F_0 and s_0 in eq 34 are equal to the free energy and average degree of dissociation of an isolated PE, respectively.

2. Small PE Distances, $D \ll \kappa^{-1}$. At short separations the average degree of dissociation saturates and is independent of κ^{-1}, as can be seen in Figure 9a. The electrostatic interaction energy of the two polymers also becomes nearly independent of κ^{-1}, as can be understood from the following argument. Consider the two polymers as uniformly, oppositely charged, and parallel lines. In the limit of no screening, $\kappa = 0$, the electrostatic energy is dominated by interactions at distances of order D and smaller. At distances larger than D opposing positive and negative charges in the two polymers can be regarded as dipoles and the electrostatic interaction between them decays as $1/z^3$ where z is their distance, measured parallel to the polymers. As long as $\kappa^{-1} \gg D$ screening affects only these dipole−dipole interactions, but not the main electrostatic contribution coming from interactions at distances smaller than D. The independence of both $\langle s \rangle$ and the electrostatic energy on κ^{-1} leads to the behavior seen at these small separations.

3. Large PE Distances, $D \gg \kappa^{-1}$. At large separations the free energy approaches the sum of free energies of the two isolated polymers. More precisely, the average degree of dissociation on the two polymers approaches a constant and the free energy can be approximated as follows

$$\frac{F}{N} \approx \frac{2F_0}{N} - 2l_B\left(\frac{s_0}{a}\right)^2 K_0(\kappa D) \qquad (34)$$

where F_0 and s_0 are the free energy and average degree of dissociation of a single, isolated PE, respectively. These constants are unrelated to the interaction between the two PEs but depend strongly on κ. The modified Bessel function $K_0(\kappa D)$ characterizes the electrostatic interaction between two parallel and uniformly charged rods:

$$K_0(\kappa D) = \int_0^\infty dz \frac{\exp(-\kappa\sqrt{z^2 + D^2})}{\sqrt{z^2 + D^2}} = \int_0^\infty du \frac{\exp(-\sqrt{u^2 + \kappa^2 D^2})}{\sqrt{u^2 + \kappa^2 D^2}} \qquad (35)$$

Deviations from the asymptotic form (34) are expected to occur only when the average degree of dissociation deviates from s_0. This happens approximately when $D \lesssim \kappa^{-1}$, as can be seen in Figure 10, where the difference between F/N and eq 34 is plotted for the same four values of κ^{-1} as in Figure 9.

B. Nonuniform Mean-Field Approach. In the case of stronger interactions between monomers within each polymer, the dissociation curve of a single PE is characterized by a plateau. In this case we expect a symmetry breaking transition with two sublattices on each PE. To deal with this case, the mean-field Hamiltonian can be generalized to account for sublattices on each one of the two PEs:

$$\mathscr{H}_0 = h_0^{\mathrm{a}}\sum_i \tilde{s}_{2i}^{\mathrm{a}} + h_1^{\mathrm{a}}\sum_{\tilde{i}} \tilde{s}_{2i+1}^{\mathrm{a}} + h_0^{\mathrm{b}}\sum_i \tilde{s}_{2i}^{\mathrm{b}} + h_1^{\mathrm{b}}\sum_{\tilde{i}} \tilde{s}_{2i+1}^{\mathrm{b}} \quad (36)$$

The mean-field equations and free energy are found using the Gibbs variational principle, in a fashion similar to that for the single polymer case. For example, the equation for h_0^{a} is

$$h_0^{\mathrm{a}} = \tilde{\mu}^{\mathrm{a}} + J\langle\tilde{s}_0\rangle_0^{\mathrm{a}} + K\langle\tilde{s}_1\rangle_0^{\mathrm{a}} + I_0\langle\tilde{s}_0\rangle_0^{\mathrm{b}} + I_1\langle\tilde{s}_1\rangle_0^{\mathrm{b}} \quad (37)$$

where $\langle\tilde{s}_i\rangle_0^{\alpha} = -\tanh h_i^{\alpha}$. Similar equations are obtained for h_1^{a}, h_0^{b}, and h_1^{b}. The coefficients J, K, I_0, and I_1 in eq 37 are equal to

$$J = \frac{1}{4}\sum_{i\neq 0} v_{\mathrm{DH}}(2ia)$$

$$K = \frac{1}{4}\sum_{i} v_{\mathrm{DH}}[2(i+1)a]$$

$$I_0 = \frac{1}{4}\sum_{i} v_{\mathrm{DH}}[\sqrt{(2ia)^2 + D^2}]$$

$$I_1 = \frac{1}{4}\sum_{i} v_{\mathrm{DH}}[\sqrt{(2i+1)^2a^2 + D^2}] \quad (38)$$

and $\tilde{\mu}^{\mathrm{a}}$, $\tilde{\mu}^{\mathrm{b}}$ are given by eqs 30 and 31. The four equations for h_i^{α} typically have multiple solutions; For example, if symmetry breaking occurs on both polymers, the number of solutions is 9. In the limit of noninteracting polymers, $I_0 = I_1 = 0$, four of these solutions are equivalent minima of the free energy, related to each other by exchange of the two sublattices on one or both of the polymers. Interactions between the polymers break the symmetry of exchanging only the sublattices in one of the polymers, and there are two (equivalent) global minima of the free energy.

1. Results. As a concrete example we consider again the model shown in Figure 3, which accounts for a low dielectric constant of the polymer backbone. Parameters are similar to Figure 4, $b = 0$, $a = 3.5$ Å, $d = 2.5$ Å, and $\kappa^{-1} = 100$ Å. The pH, pK_{a}, and pK_{b} values are chosen such that pH $-$ pK_{a} $=$ pK_{b} $-$ pH $= 3$. The coefficients J and K are set as in Figure 4 with $\kappa^{-1} = 100$ Å, $J = 1.4$, and $K = 5.8$. For the coefficients I_0 and I_1 we use eq 38 with the screened Debye−Hückel interaction in water, eq 4. Both of these choices are approximations that become inaccurate when the polymers are very close to each other, because the electrostatic Green's function should then be evaluated in the presence of two dielectric cylinders. However, we expect our results to be qualitatively correct, as will be further discussed below.

Figure 11 shows the average charging of the two polymers as a function of their separation D. Due to the plateau in the dissociation curve of each polymer, $\langle s\rangle$ is close to $^1/_2$ in most of the separation range. A sharp increase in $\langle s\rangle$ is found at close separations of a few Angströms. Note that in this range, where interactions between the polymers affect the average charging, the distance is much smaller than the Debye length, $\kappa^{-1} = 100$ Å.

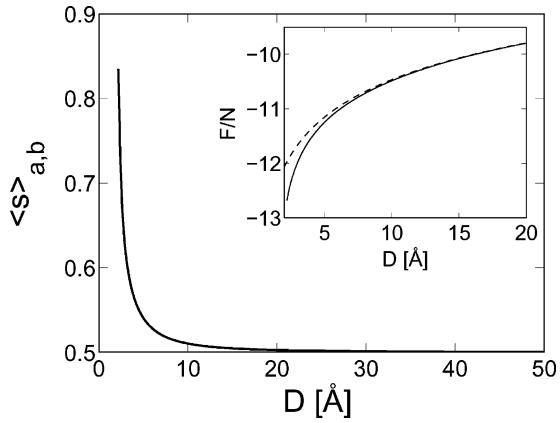

Figure 11. Average degree of dissociation of interacting polyacid and polybase, as a function of their distance. The interactions between monomers within each PE are calculated by assuming a low dielectric backbone, as in Figure 3. The parameters of the model are as in Figure 4: $a = 3.5$ Å, $d = 2.5$ Å, $b = 0$, $\kappa^{-1} = 100$ Å, and pH $-$ pK_{a} $=$ pK_{b} $-$ pH $= 3$. The inset shows the free energy per monomer, F/N, as a function of D (solid line). The dashed line shows the approximation of eq 34 with $s_0 = ^1/_2$ and F_0 set to match the value of F at large D.

The inset shows the free energy (solid line) as function of a D. For comparison we show (by a broken line) the approximation of eq 34, with s_0 equal to $^1/_2$ and F_0 matching the value of F at large D. The two free energies deviate from each other only at very small distances, where $\langle s\rangle$ is larger than 1/2.

In summary, the symmetry-broken solution is stable for a wide range of distances and gives way to a symmetric solution only at very small distances. Note that in Figure 11 the most significant increase in $\langle s\rangle$ is found for $D < 5$ Å, where the two cylinders overlap. However, with the dielectric discontinuity on both polymers taken properly into account (affecting I_0 and I_1 as well as K and J), we can expect a stronger interaction between the polymers for small D. This will lead to an increase of the average charging at larger values of D than in Figure 11.

IV. Summary

The main result in the first part of this work concerns a generalization of the standard mean-field theory of charge regulation in weak PEs. The polymer is divided into two sublattices, allowing explicitly for correlations between these sublattices to be taken into account. Similar models have been studied in the past in the context of Ising-like models. In the Ising model, interactions are usually assumed to be short-range. If only interactions between neighboring monomers are considered, the partition function can be calculated exactly. For PEs the main advantage of using a mean-field approximation is that it allows long-range electrostatic interactions to be taken into account. Simultaneously, one expects mean-field methods to gain in accuracy as the range of interactions increases. Our main result is that a mean-field approach with separation into two sublattices is adequate within a wide range of model parameters. In particular, it succeeds in the case of large intermonomer interactions, where a uniform mean-field theory fails, while also taking into account long-range interactions, which may still play an important role.

A motivation for the use of a nearest-neighbor approximation was recently suggested in ref 4. It was pointed out that a low dielectric constant of the polymer backbone can lead to strong enhancement of the coupling between close-by monomers. We show that even within the model of ref 4, the nearest-neighbor approximation needs improvement for large values of the Debye length, because of the contribution of interactions between non-

neighboring monomers. On the other hand, a mean-field approximation with two sublattices is semiquantitatively accurate. We also demonstrate that effects due to the dielectric discontinuity between the PE interior and the aqueous solvent depend sensitively on the location of the charged groups within the low-dielectric cavity; this is quite relevant, because for most experimental PE architectures, the charged groups are not located centrally but are displaced toward the aqueous interface.

The linearized Debye−Hückel theory is used in this work to evaluate the interaction between monomers. This, of course, is only an approximation, whereas in principle, the full nonlinear response of the ionic solution must be taken into account. Use of Debye−Hückel interactions is justified as long as the electrostatic potential is small compared to the thermal energy. Hence this approximation is probably reasonably accurate in the plateau region, where the average charge along the polymer is small. Far away from the plateau, and for highly charged PEs, one needs to go beyond Debye−Hückel theory, using the nonlinear Poisson−Boltzmann theory. The great advantage of using pairwise interactions is that they allow tractable, analytic solutions to be obtained. In contrast, the nonlinear distribution of ions cannot be calculated analytically even near a uniformly charged cylinder immersed in a salt solution, let alone an inhomogeneously charged PE. In light of this situation we believe that the results presented in this work provide a useful qualitative treatment of charge regulation even for the case of highly charged PEs, although they may be quantitatively modified by charge renormalization due to nonlinear effects close to the PE.[17]

In the second part of this work we studied the interaction between a polyacid and a polybase, using a mean-field approximation. This interaction leads to an increase of the average charging in both polymers as they approach each other. In addition, the interaction energy between a weak polyacid and a weak polybase is stronger than expected in the absence of distance-dependent charge regulation. This means that the effect of charge regulation may be important for the building of stable multilayers, because it decreases the repulsion between similarly charged weak PEs (because the charge regulation in this case decreases the charge strength) and at the same time leads to strongly bound polyacid−polybase pairs. For close-by polymers the electrostatic energy is dominated by interactions between neighboring monomers, and the free energy depends only weakly on the Debye screening length κ^{-1}. On the other hand at large separation between the polymers both the average degree of dissociation and the free energy typically vary strongly with κ^{-1}. The characteristic distance where interactions between the polymers can affect their degree of dissociation is the Debye screening length. However, when there is a plateau in the charge vs pH curve of a single PE, the degree of dissociation may remain close to $^1/_2$ even at small separations compared to κ^{-1}. In these cases a sharp increase in the average dissociation can occur close to contact.

The increase of charging when weak polyacids and weak polybases come into contact could in principle be observed using infrared spectroscopy in multilayers. However, one has to keep in mind that in such highly concentrated systems the oppositely charged groups will get very close to each other and form salt bridges.

Acknowledgment. Y.B. thanks the Minerva foundation for a grant. This work was financially supported by Deutsche Forschungsgemeinschaft (DFG, SFB 486) and the Fonds der Chemischen Industrie.

References and Notes

(1) Raphael E.; Joanny J.-F. Annealed and quenched polyelectrolytes. *Europhys. Lett.* **1990**, *13*, 623−628.

(2) Borukhov, I.; Andelman D.; Borrega, R.; Cloitre M.; Leibler L.; Orland H. Polyelectrolyte titration: theory and experiment. *J. Phys. Chem. B* **2000**, *104*, 11027−11034.

(3) Zito T.; Seidel C. Equilibrium charge distribution on annealed polyelectrolytes. *Eur. Phys. J. E* **2002**, *8*, 339−346.

(4) Borkovec, M.; Daicic, J.; Koper, G. J. Ionization properties of interfaces and linear polyelectrolytes: a discrete charge Ising model. *Physica A* **2002**, *298*, 1−23.

(5) Decher, G. Fuzzy Nanoassemblies: Toward layered polymeric multicomposites. *Science* **1997**, *277*, 1232−1237.

(6) Sukhorukov G. B.; Donath E.; Davis S. A.; Lichtenfeld H.; Caruso F.; Popov V. I.; Möhwald H. Stepwize polyelectrolyte assembly on particle surfaces: a novel approach to colloid design. *Polym. Adv. Technol.* **1998**, *9*, 759−767.

(7) Caruso F.; Caruso R. A.; Möhwald H. Nanoengineering of inorganic and hybrid hollow spheres by colloidal templating. *Science* **1998**, *282*, 1111.

(8) Yoo, D.; Shiratori, S.; Rubner, M. Controlling bilayer composition and surface wettability of sequentially adsorbed multilayers of weak polyelectrolytes. *Macromol.* **1998**, *31*, 4309−4318.

(9) Shiratori, S.; Rubner, M. pH-dependent thickness behavior of sequentially adsorbed layers of weak polyelectrolytes. *Macromolecules* **2000**, *33*, 4213−4219.

(10) Netz, R. R. Charge regulation of weak polyelectrolytes at low- and high-dielectric-constant substrates. *J. Phys.: Condens. Matter* **2003**, *15*, S239-S244.

(11) Huang, K. *Statistical Mechanics*, 2nd ed.; Wiley: New York, 1987.

(12) Marcus, R. A. Titration of polyelectrolytes at higher ionic strengths. *J. Phys. Chem.* **1954**, *58*, 621−623.

(13) Harris, F. E.; Rice, S. A. A chain model for polyelectrolytes. I. *J. Phys. Chem.* **1954**, *58*, 725−732.

(14) Lifson, S. Potentiometric titration, association phenomena, and interaction of neighboring groups in polyelectrolytes. *J. Chem. Phys.* **1956**, *26*, 727−734.

(15) Baxter, R. J. *Exactly solved models in statistical mechanics*; Academic Press: London, 1982.

(16) Netz, R. R. Debye−Hückel theory for interfacial geometries *Phys. Rev. E* **1999**, *60*, 3174−3182.

(17) Netz, R. R.; Orland, H. Variational charge renormalization in charged systems. *Eur. Phys. J. E* **2003**, *11*, 301−311.